Progress In Electromagnetics Research C, Vol. 69, 169–179, 2016

Design of Continuous Beam Steerable and Scalable Unit Module for Wireless Power Transmission Using Injection-Locked Oscillator Array

Ce Zhang[1], Bingnan Wang[2, *], and Koon Hoo Teo[2]

Abstract—Long-range wireless power transmission (WPT) is implemented with the beamforming using the phased array transmitter technology, which has been extensively applied in the radar systems. The cost of a conventional phased array transmitter module scales up in proportion to the number of antenna elements, as the massive number of transmit channels results in the increasing complexity of hardware and feeding antenna elements. Besides, the conventional phase-shifting transmitter architecture has lower DC to RF power conversion efficiency due to the insertion loss of power combining network at microwave frequency. In this paper, the concept of spatial power combining transmitter is utilized, and the upconversion circuit is greatly simplified to an injection locked oscillator. Our WPT system is implemented with the technology of oscillator array antenna at 2.4 GHz, which converts DC power to RF power and radiates into the air directly. The feedback voltage controlled oscillator (VCO) is implemented as the microwave source using a off-the-shelf bandpass filter, and the external signal is injected to the oscillator via a microstrip coupler. The oscillator core shows the DC-to-RF conversion efficiency of 45.87% with the injected power of 0 dBm at 2.4 GHz. Then the digital phase shifter is used to phase shifting the injected signal to extend the beam coverage. From the link budget analysis, the overall DC-to-DC efficiency of our highly-integrated system shows 1.5 times (0.22%) of the conventional phased array (0.15%) when the separation between the transmit array and the receive horn antenna is 1.2 meters. Therefore, as an modularized array, the proposed system demonstrates the promising capability of upscaling to an efficient massive array with greatly reduced bill-of-materials (BOM).

1. INTRODUCTION

Microwave power transmission has its unique advantages for its ability to supply power to not-accessible and mobile receivers and is also called long-range wireless power transmission (WPT). The implementation of long-range WPT requires the phased array transmitter technology, in order to achieve the reasonable transmission efficiency with high array gain and beam steering capability to mobile power receivers [8–10].

The active integrated antenna (AIA) technology is a low-cost substitute of conventional phase-shifting array architecture. It is a well-established technology allowing high-level integration of antenna radiators and microwave nonlinear elements. The driving force of AIA technology is to combat the challenges at microwave and millimeter-wave frequency including the high insertion loss of transmission line, the limited output power of active elements, and the high cost of high-performance phase shifters. There are several variations of oscillator based AIA technology as reviewed by [12]. The injection locking techniques have been widely used in AIA design and can be used to achieve the synchronous operation of oscillators and phase coherent power combining. The simplicity of phase shifting circuitry also reduces the complexity of beamforming and leads to a low cost phased array implementation of WPT system.

Received 18 August 2016, Accepted 3 November 2016, Scheduled 23 November 2016

* Corresponding author: Bingnan Wang (bwang@merl.com).

[1] Department of Electrical Engineering, University of Washington, Seattle, WA 98195, USA. [2] Mitsubishi Electric Research Laboratories, Cambridge, MA 02139, USA.

The injection locked oscillator array (ILOA) with a conventional feed gives better phase noise performance and the consequent less leakage to adjacent channels, which is critical if the active array system delivers wireless power at the single tone in ISM band. The voltage controlled oscillator (VCO) is the core of ILOA design as each array element is allocated with a self-contained voltage-controlled oscillator. The oscillators are all governed by a common signal at desired frequency of operation, which can be distributed with a corporate feed network [2] or optical carrier via photodetector [5]. Two oscillator configurations can be generalized for microwave oscillator design using three-terminal transistors: series feedback and parallel feedback [6]. The series feedback topology is more suitable for wideband oscillation generation while the parallel feedback topology is more suitable for narrowband signal generation like WPT system for its lower phase noise with the insertion of high quality factor resonator [3, 11]. Therefore, this paper presents a unit of injection-locked antenna array and demonstrate that such a small unit can be scaled up to large scale array to implement a WPT system that meets the system requirement with reduced bill-of-materials (BOM). To extend the beam coverage, the switched line digital phase shifter is designed and co-simulated with the unit module.

In this paper, we present a prototype of wireless power transmitter using injection-locking oscillator array with improved coverage and demonstrate that such a small unit can be scaled up to a large array that meets the WPT system requirement with reduced bill-of-materials (BOM).

2. DESIGN OF INJECTION-LOCKED VCO

The VCO is the core of the following proposed low-cost antenna array implementations for WPT RF system. The parallel feedback topology of microwave oscillator is chosen to operate as microwave source for radiators in the two proposed antenna array implementations because the narrowband signal generation with lower phase noise is required in wireless power delivery. To further enhance the phase noise, an external high purity signal is injected into the feedback oscillator.

The block diagram is shown in Fig. 1(a), and the detailed sub-circuit is shown in Fig. 1(b). The feedback loop consists of four components to assure the oscillation at the desired frequency f_0: amplifier, microstrip coupler, band pass filter and phase shifter. The amplifier converts the DC power to RF power and sustains the oscillation while the oscillation is determined by the feedback loop. The feedback oscillator is integrated with the four port microstrip coupled line structure, which provides the positive feedback to the amplifier by coupling the output of the amplifier to its input path. The high quality factor band pass filter in the loop passes the signal in the frequency band of interest while attenuates the out of band signals so the loop only satisfies the Barkhausen Criterion (closed loop gain is greater than unit and the phase shift is 180°). Besides, since the microstrip coupled line isolates the opposite port on the coupled line and passes a portion of signal power on the through line, the remaining two of four ports coupled line can be used for feeding antenna and injecting the external signal. In Section 3, the ILOA requires the use of VCO to generate the phase shifting at each element so the loaded line phase shifter is inserted into the loop. This phase shifter implements the tuning of closed loop phase shift and, as a consequence, the oscillation frequency. The loop gain of the oscillator core can be expressed concisely as follows.

$$A_{cl}(f_0) = \alpha G_{amp} G_{PS} G_{BPF} K_{coupling} \tag{1}$$

where G_{amp} is complex amplifier gain; G_{PS} is the S_{21} of phase shifter; G_{BPF} is the S_{21} of BPF; α includes the propagation attenuation and phase shift of the routing; $K_{coupling}$ is coupling coefficient of the coupled line.

2.1. Amplifier

The amplifier is implemented with the PHEMT transistor ATF-34143 from Avago Technology and fabricated on a 58 mil thickness double layer FR4. The transistor is biased at $V_{gs} = -0.6\,\mathrm{V}$ and $V_{ds} = 1\,\mathrm{V}$ with two grounded source terminals, and this bias condition gives the simulated small signal gain of 14.73 dB using the nonlinear model from Avago. The transistor converts the DC power to RF power under the oscillation condition, which is set by the feedback loop connecting from the drain to the gate terminal via microstrip coupler, bandpass filter, and loaded line phase shifter. The drain current

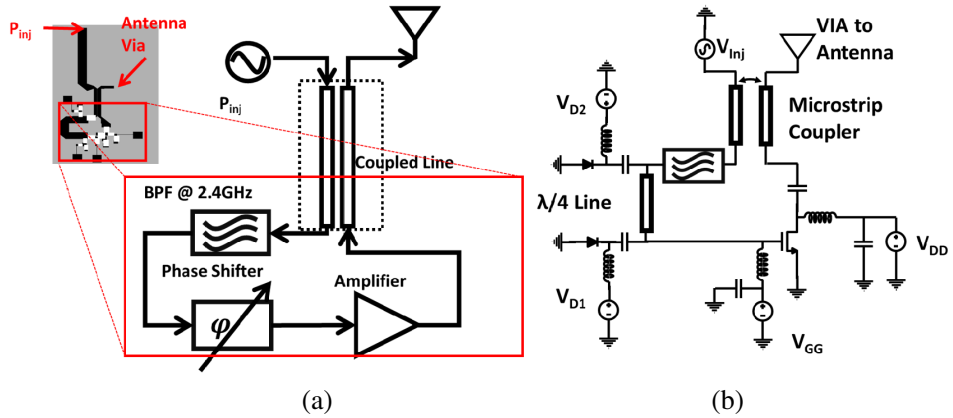

(a) (b)

Figure 1. (a) Block diagram of the oscillator. (b) Schematic diagram of the oscillator.

of the amplifier is measured as 28.06 mA under this bias condition so the DC power consumption of each oscillator element is 84.18 mW.

2.2. Microstrip Line Coupler

The microstrip line coupler has four ports and fabricated on the circuit board. The drain output and the gate input are connected to two coupled ports as in Fig. 1. The coupling coefficient between these two coupled ports is intentionally made as high as −1.63 dB at 2.4 GHz at the cost of high insertion loss (−5.71 dB at 2.4 GHz) from drain output to antenna input port. This design choice results from the high sensitivity of amplifier gain to gate bias V_{gs}. When the gate bias is off the chosen voltage $V_{gs} = -0.6$ V, the gain of amplifier drops to around 10 dB. The low amplifier gain can not ensure that the loop gain is greater than unity because the insertion of feedback route on lossy FR4, bandpass filter, and phase shifter attenuates the feedback signal from output to input significantly. However, since the coupled signal from drain to gate is cycled to sustain the oscillation rather than dissipated by the substrate, the higher insertion loss from drain output to antenna port only doesn't increase the power dissipation and lower the oscillation efficiency by the same amount.

2.3. Bandpass Filter

The microwave power is transmitted to the receiver wirelessly via continuous wave signal, so the purity of generated microwave signal is a critical parameter for the oscillator design, which is related to the phase noise of oscillators. The most common low phase noise oscillator integrates with single high-quality-factor (high-Q) resonator such as dielectric resonator [6]. The microwave oscillator achieves the frequency stabilization with the employment oft these high-Q resonators as a popular technique in the series feedback configuration [3]. The microwave oscillator can also be implemented by placing the bandpass filter in the feedback path for frequency selection in the parallel feedback configuration.

In the previous studies, the planar microwave oscillator implements the bandpass filter with a variety of microstrip line filters [4, 11]. However, this technique is not used in our design because the requirement of loop gain requires low insertion loss in the loop given the lossy substrate. It is difficult to ensure a low insertion loss with high selectivity of the filter as the higher order filter ensures the narrow bandwidth at the cost of more sections of the microstrip line. For this reason, in our design, the commercial off-the-shelf (OTS) bandpass filter is employed to achieve the same functionality with lower insertion loss and smaller footprint.

Despite the loss of the freedom of optimizing the bandpass filter, the same filter design process can be applied to the selection of the filter from the manufacturers. The Leeson's phase noise model Eq. (2) shows that the output spectrum of an oscillator is a function of spectrum quality factor (Q_s) [7].

$$S_\phi(\delta\omega) = S_{\Delta\theta}\left[1 + \frac{\omega_0}{2Q_s\delta\omega}\right] \tag{2}$$

where $\delta\omega$ is the offset frequency from the oscillation frequency ω_0, $S_{\Delta\theta}$ the additive noise component, and the Q_s the spectrum quality factor. The quality factor can be expressed in terms of group delay, which relates to the phase response of filter (Eq. (3)).

$$Q_s = \frac{\omega_0 \tau_d}{2} \tag{3}$$

where $\tau_d = \left|\frac{d\phi(\omega)}{d\omega}\right|_{\omega=\omega_0}$ is the group delay of the filter.

Most papers about low phase noise oscillator focus on maximizing the spectrum quality factor, which is equivalent to the group delay or the sharpness of phase frequency. The bandpass filter demonstrates peaking group delay at the edge of the passband and, therefore, the oscillation is designed to occur at the transition region using tailored planar microstrip filter. In [4], the Phase Noise Figure-of-Merit (PNFOM) is used to include the both group delay response and insertion loss and evaluate the performance of band pass filter. By placing the oscillation in the band transition of the planar filter, the frequency, at which the PNFOM is minimized, is utilized to achieve the low phase noise oscillator. Several OTS bandpass filters are evaluated with the frequency dependence of phase response. The (Fig. 2(a)) and the spectrum quality factor (Fig. 2(b)) show the frequency dependent group delay of several available bandpass filters by Johanson Technology.

$$\text{PNFOM} = 10 \cdot \log\left(\frac{L}{\tau_d^2}\right) \tag{4}$$

$$Q_{sc} = \frac{\omega_0}{2}\frac{d}{d\omega}\left(\ln\left|\frac{z_{11}}{z_{12}}\right|\right) + j\frac{\omega_0}{2}\frac{d}{d\omega}\left(\angle\left(\frac{z_{11}}{z_{12}}\right)\right) \tag{5}$$

where z_{11} and z_{12} are the matrix elements of the two port impedance matrix $[Z]$ of the filter.

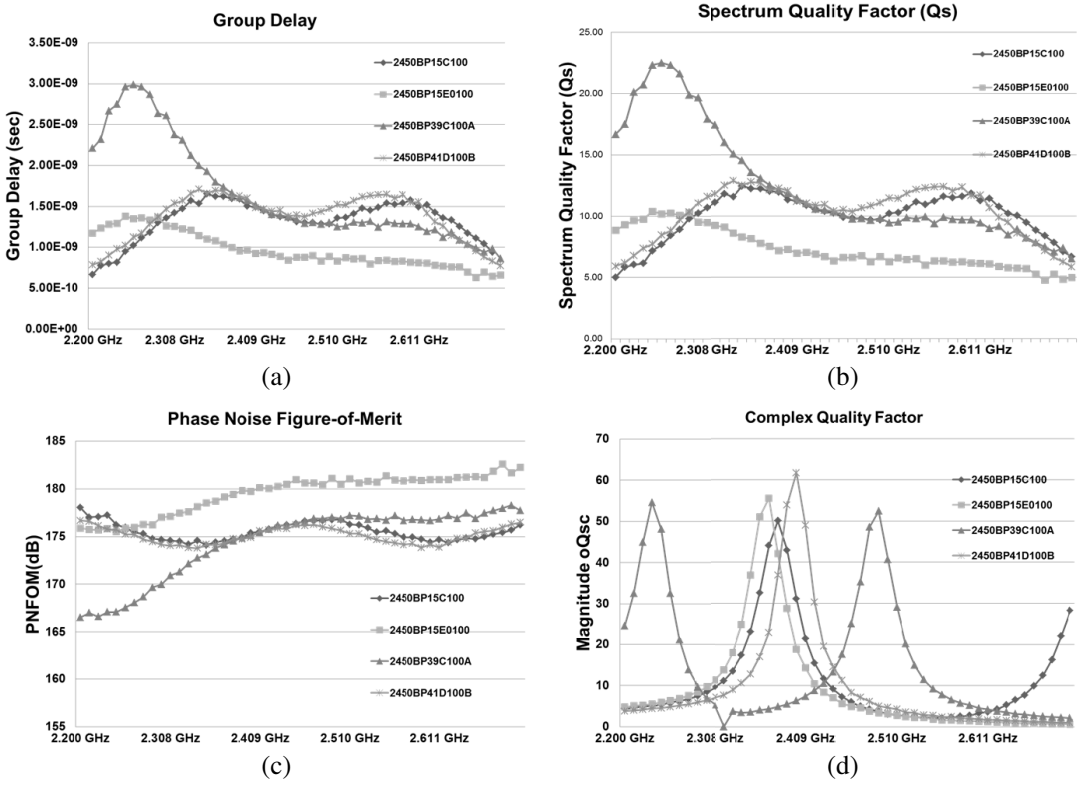

Figure 2. Characteristics of bandpass filter: (a) Group delay of selected OTS bandpass filter. (b) The spectrum quality factor of selected OTS bandpass filter. (c) The phase noise figure-of-merit of selected OTS bandpass filter. (d) The complex quality factor of selected OTS bandpass filter.

However, in most communication systems, the group delay should be as flat as possible to minimize the distortion of signals so the OTS filter, designed for the WiFi/Bluetooth in the ISM band, does not give the peaking of quality factor as the tailored planar microwave oscillator within the operation band. Although these bandpass filters don't show the sharp phase response within the operation band, the out-of-band amplitude attenuation still gives the frequency selectivity and the amplitude response is not included in either PNFOM or group delay/quality factor. For this reason, the paper [11] introduces the complex quality factor (Eq. (5)) to evaluate the characteristics of the selected filters. To find out the performance of the bandpass filters available in the market, the selected commercial filters are simulated for comparison. The evaluation is carried out with PNFOM and complex quality factor, which are shown in Fig. 2(c) and Fig. 2(d), respectively.

From the PNFOM and complex quality factor, the models 2450BP41D100B and 2450BP15C100 by Johanson Technology are the two potential choices of the bandpass filter for better phase noise performance at the oscillation frequency around 2.4 GHz. Therefore, these two models are chosen for the study of phase noise with Harmonic Balance (HB) simulation engine.

2.4. Phase Shifter

The parallel feedback loop ensures the oscillation within frequency band, while in this paper, the voltage-controlled frequency of oscillation is required for the phase tuning of ILOA design. To implement this function, the frequency of satisfying oscillation condition has to be tuned by an external control voltage. The 180° phase shift can be easily tuned to a different frequency with the simple phase shifter while the loop gain is almost intact if the insertion loss is low enough. There are several ways of implementing the phase shifter such as reflection type, loaded line and switched line phase shifter.The load phase shifter achieves a phase shift of less than 45 degrees with the lower insertion loss by creating a perturbation in the phase of the signal with only a small effect on the amplitude of the signal. Therefore, the loaded line phase shifter is used in our design, where the high impedance load is implemented with a voltage controlled varactor diode SMV2020 by Skyworks. Two varactors are loaded in parallel with input and output of quarter wave transmission line via a 33 pF series capacitance, which is short at oscillation frequency and shields the DC control voltage from the feedback path.

The return loss of loaded line phase shifter works for a broadband operation while the insertion loss (Fig. 3(b)) determines the phase tuning range because when the parallel impedance is small, the insertion loss is too high to ensure the loop gain greater than unity. Therefore, the insertion loss is set to below 1.5 dB at 2.4 GHz and this limit determines the maximum diode varactor voltage of 8V. The phase shift is plotted in Fig. 3(a) for the diode varactor voltage within this limit and the phase tuning range is also presented at center frequency 2.4 GHz in Fig. 3(d).

2.5. Oscillator

The aforementioned elements are connected into a closed loop to build a VCO elements. The integral closed loop system is interfaced with the external injection source and antenna element via the microstrip line coupler. In the mode of VCO, the port of injection signal is matched while the antenna port is connected to the antenna feed.

The closed loop gain is presented as in Fig. 4(c) with the varactor diode voltage of 0 volts. The loop gain shows that the loop gain can only be greater than unity from 2.3 GHz to 2.55 GHz due to the attenuation of bandpass filter while the phase of loop gain determines the frequency of oscillation. Therefore, the loaded line phase shifter enables the tuning of the oscillation frequency by changing the phase shift of feedback loop. Fig. 4(a) shows the tuning range of oscillation frequency by sweeping the varactor diode voltage from 0 to 8 volt.

From the discussion about bandpass filter, the phase noise is determined by the parameters of the bandpass filter. Thus, the phase noise of feedback oscillator with different models is simulated as in Fig. 4(d). This simulation shows that the simulated phase noise of oscillator with the filter 2450BP41D100B and 2450BP15C100 are better than the oscillator with the other filter and are almost the same for the offset frequency greater than 10 kHz. However, the filter 2450BP15C100 shows better performance if the offset frequency is small. This simulation result leads to our choice of 2450BP15C100

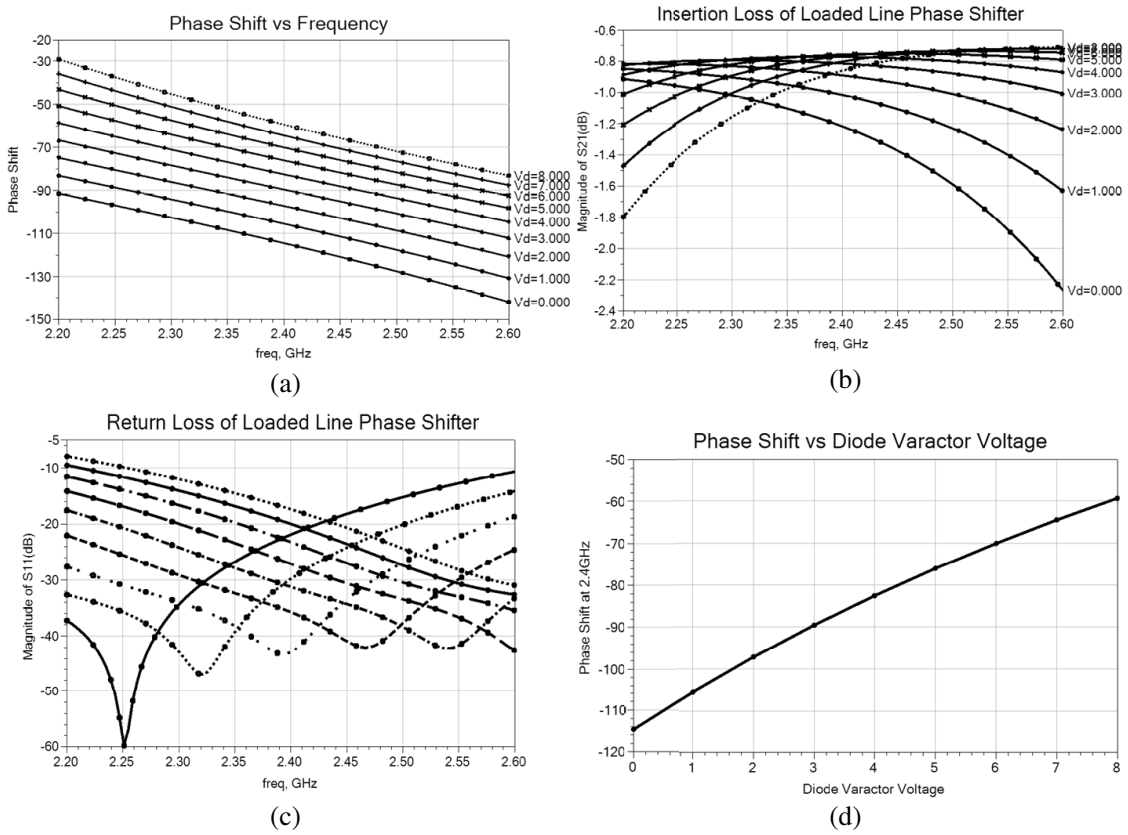

Figure 3. Characteristics of loaded line phase shifter: (a) Phase shift of the loaded line phase shifter. (b) Insertion loss of the loaded line phase shifter. (c) Return loss of the loaded line phase shifter. (d) Phase shift at 2.4 GHz over diode varactor voltage.

in the construction of low phase noise voltage controlled oscillator. Such oscillator design gives the phase noise of −78.58 dBc/Hz at 1 kHz offset and −142.83 dBc/Hz at 1 MHz offset.

3. DESIGN OF SCALABLE INJECTION-LOCKED OSCILLATOR ARRAY

The phases of the antenna outputs are not synchronized until a common external signal is injected to the microstrip line coupler. Then the VCO elements become a group of synchronized source and are locked to the frequency of injected signal instead of its free running frequency. This phenomenon of injection locking is called frequency entrainment and arises from the observations of synchronized mechanical pendulum. This phenomenon can be described by a simply tuned oscillator model and Adler's equation (Eq. (6)) proposed by Adler in [1].

$$\frac{d\phi}{dt} = \omega_0 - \omega_{inj} + \Delta\omega_m \sin(\psi - \phi) \tag{6}$$

where $\Delta\omega_m = \frac{V_{inj}}{V_{osc}} \frac{\omega_0}{2Q}$ is called the locking range, which is the maximum allowable frequency offset between the oscillation frequency and the injected frequency. ω_0 is the free-running oscillation frequency, V_{osc} the free-running oscillation amplitude, Q the quality factor of the oscillator, V_{inj} the amplitude of the injected signal, and ψ and ϕ are the phase of the injected signal and phase of the output signal.

The output phase of each oscillator is related to the difference between the frequency of the injected signal and the free-running frequency of the oscillator at the steady state. The phase shift can be controlled by tuning the oscillation frequency of VCO rather than conventional changing the state of phase shifters. The mathematical expression of phase shift relative to the injected signal is described

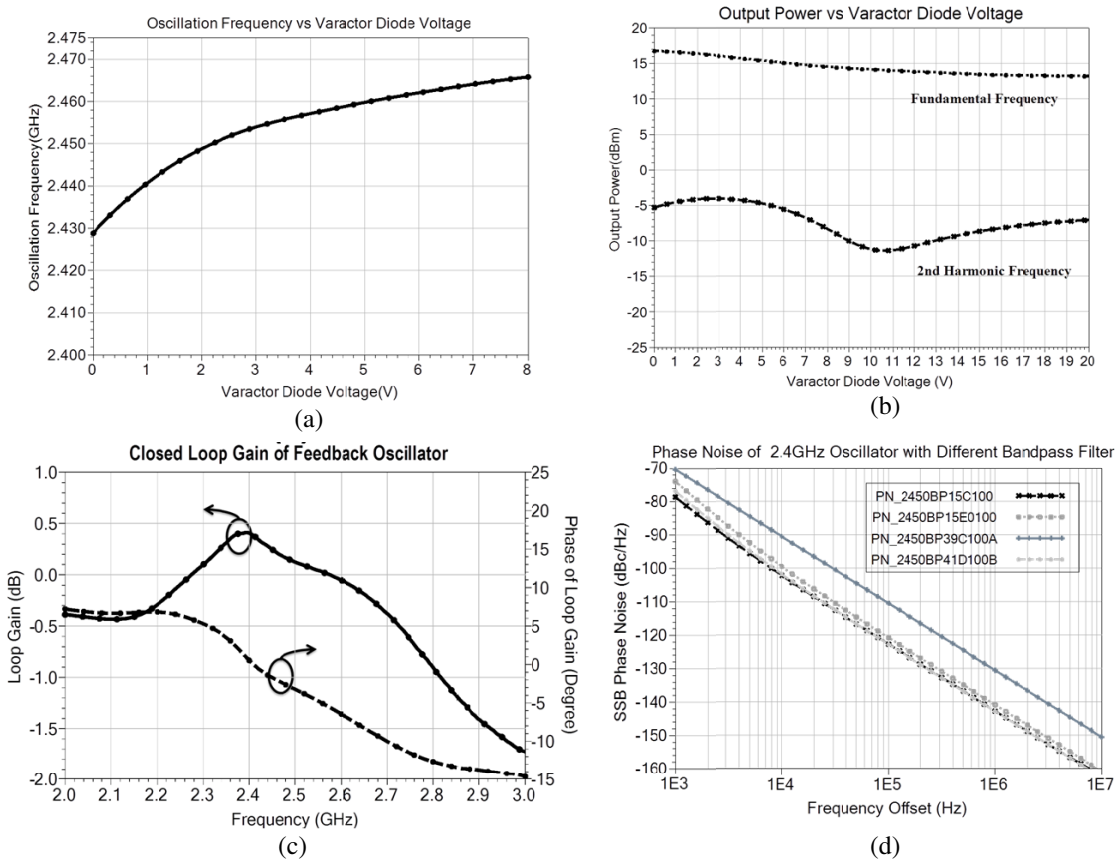

Figure 4. Characteristics of VCO: (a) Oscillation frequency of voltage controlled feedback oscillator. (b) The output power of a single oscillator unit with sweeping varactor diode voltage. (c) Closed loop gain of feedback oscillator. (d) Phase noise of feedback oscillator.

by the equation (Eq. (7)) in [12].

$$\psi - \phi = \sin^{-1}\left(\frac{\omega_0 - \omega_{inj}}{\Delta\omega_m}\right) \tag{7}$$

The VCO described in Section 2 is integrated with the microstrip patch antenna through a via feed. The antenna port of microstrip line coupled is connected to the feed point of the patch antenna directly, in order to shorten the insertion loss of the feed line. The position of feed point is tuned to reduce the mismatch loss at the port. In this way, the synchronized microwave power sources are combined coherently in space, as called spatial power combining, has many advantages over the on-board power combining such as high linearity, low loss, and compact layout footprint.

As the phase tuning of each antenna element is equivalent to the oscillation frequency control with a varactor, the performance of the designed oscillator is shown by sweeping varactor diode voltage in Fig. 6(b). The plot shows that the phase tuning range of each oscillator is up to 41 degrees. The equation (Eq. (7)) also implies the limit of the scanning angles because the phase shift with injection locking cannot be out of the range $-90° < \psi - \phi < 90°$. Normally, the N-element ILOA has implemented with linear phase progression and tunes the oscillation frequency according to (Eq. (7)) to yield a linear phase step between adjacent elements. Under this condition, the maximum interelement phase difference can be readily computed as $180°/(N-1)$. The WPT requires the large scale integration of phased array elements, whereas the maximum scanning angle is significantly limited as with the increase in the number of antenna elements.

To extend the phase tuning range, the externally injected signal to each oscillator is phased with phase shifter as in Fig. 5(a). The digital phase shifter is more popular in modern passive phased array

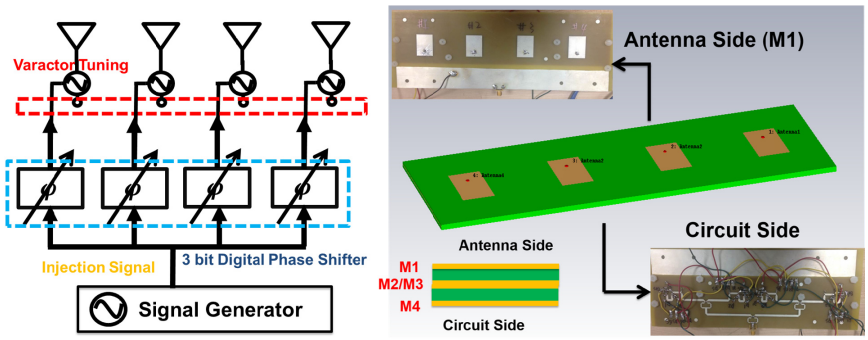

(a) (b)

Figure 5. (a) The system of injection-locked oscillator array. (b) Stack-up of antenna array.

system because of its immunity to on their voltage control lines. However, since the cost of digital phase shifter increases dramatically as with the increase of bit resolution, one drawback of the low-cost digital phase shifter is the inability of continuous beam scanning. The proposed system enables the continuous beam scanning with the low-resolution digital phase shifter in a simple way. The digital phase shifter introduces the phase shift of the injection signal and determines the coarse angle of beam steering, whilst the relative phase shift between each element and injected signal is controlled based on the injection locking principle and used for fine tuning. Moreover, because the injected signal is to lock the oscillator, the nonlinearity of digital phase shifter is a less significant problem as it is in the conventional phased array that amplifies the signal out of phase shifter.

4. RESULTS AND DISCUSSIONS OF INJECTION-LOCKED OSCILLATOR ARRAY

Based on the proposed design, the integration of injection locking utilizes a stack-up substrate, which has the antenna array on the top side and the RF circuit on the bottom side. The top and bottom sides are fabricated separately with the 58 mil FR4 process. Then the ground sides of the two separate circuits are attached to each other using electrically conductive adhesive. The fabricated prototype of ILOA is presented in Fig. 5(b).

4.1. Performance of Injection-Locked Oscillator Array Prototype

The fundamental frequency output power is plotted to estimate the max power delivery range and number of elements to meet the specifications. Besides, since the linearity of oscillator is a critical parameter to ensure the coexistence of WPT system and other wireless devices, the second harmonics output power is also presented in the same plot in Fig. 4(b). In addition, the drain current of the amplifier is measured as 28.06 mA, so the power consumption per oscillator is 72.18 mW. Since the RF power output out of each radiator is simulated as 33.11 mW, the DC-to-RF conversion efficiency is as high as 45.87%.

The phase shift of each oscillator unit is simulated with nonlinear model and EM extracted result in Agilent ADS. Fig. 6(a) shows that the phase tuning range depends on the injected signal power so the injected power is set to the level of 0 dBm that maximize the phase tuning range in our design. However, the maximized phase range is only 55.7 degrees and far away from the coverage of all possible directions of receivers. The radiation pattern of the designed injection-locked array (1-by-4 linear array) is presented in Fig. 7(a). As the maximum interelement phase difference is limited to $56/3 = 18.5$ degrees, the maximum beam steering angle with linear phase step is limited to the maximum theta of $\theta = \arcsin((\Delta\phi_{\max}\lambda_0)/(2\pi\Delta d)) = 5.8^\circ$.

To extend the coverage, the proposed solution in Section 3 is evaluated by integrating the oscillator unit with the designed digital phase shifter. The designed digital phase shifter is a switched line phase shifter with 3-bit resolution and controlled by PIN diode. The 3 stages of microstrip delay line are cascaded and the PIN diode is inserted in series with the transmission line. When the injection power

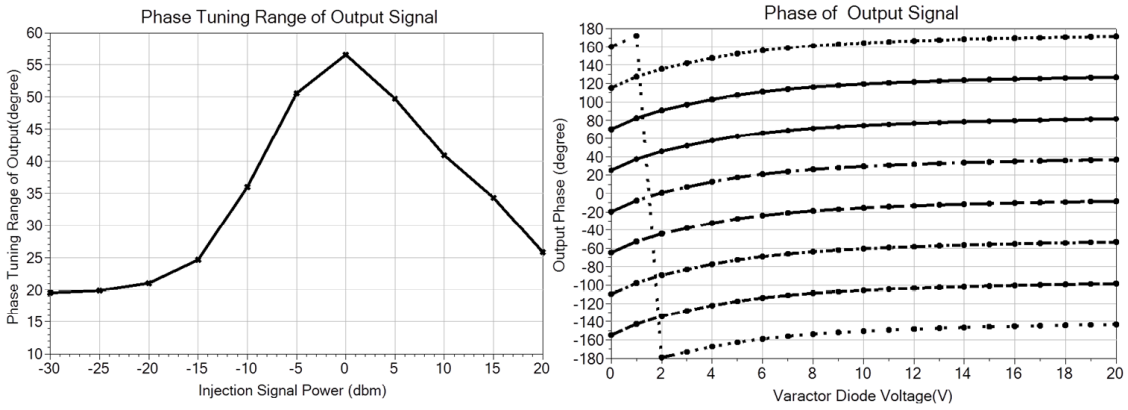

(a) (b)

Figure 6. (a) The phase tuning range vs sweeping injection signal power. (b) Phase shift of injection-locked oscillator at 2.4 GHz vs sweeping varactor diode voltage.

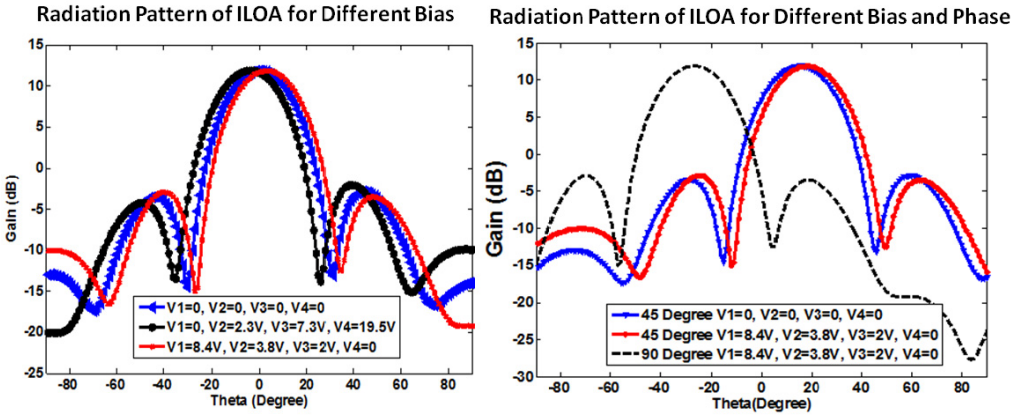

(a) (b)

Figure 7. (a) Simulated radiation pattern of injection-locked oscillator array for different bias (phi = 90 degrees). (b) Simulated radiation pattern of injection-locked oscillator array with digital phase shifter for different bias.

at the injection port of oscillator unit is tuned to 0 dBm at 2.4 GHz, the performance of integrated ILOA and digital phase shifter is simulated and shown in Fig. 6(b). This plot shows that the hybrid of injection-locked oscillator and the digital phase shifter achieves continuous phase tuning of 360 degrees. This simple digital phase shifter is simulated with the oscillator antenna array together and enable the coarse phase tuning with the digital control line. The phase response of phase shifter associated with ILOA is co-simulated and plotted in Fig. 6. The results imply that this integrated system can achieve the beam scanning to any direction in the broadside.

4.2. System Analysis of the Proposed Prototype

The experiment of WPT system is carried out in indoor environment as in Fig. 8. The distance between the transmit and receive antennas is 5 meters to ensure the operation of far field. A standard gain (11.4 dBi at 2.4 GHz) horn antenna is used as a receiver. The power consumption per oscillator is 72.18 mW while the RF power output from each radiator is simulated as 33.11 mW if 0 dBm single tone signal at 2.4 GHz is injected. The max EIRP (Effective Isotropic Radiated Power) of the proposed system is simulated as 25.9 dBm. The Spectrum Analyzer shows the RF power of −29.6 dBm, and the insertion loss of the cable and adapters from the receive antenna is measured as −11.4 dB using Network

Analyzer. If the cable loss is removed, the received RF power is −18.1 dBm. Therefore, the wireless transmission over 5-meter distance gives the estimated efficiency of 0.0052% without the RF-to-DC conversion loss.

Furthermore, another experiment includes the RF rectifier with an RF-to-DC conversion efficiency of 40% into the estimation, and the distance between transmit and receive antennas is changed to 1.2 meters to investigate the DC-to-DC transmission efficiency. The system losses of the proposed system and conventional phased array are presented in the form of a pie chart (Fig. 9), which shows the percentage of system loss. Fig. 9 shows that the overall efficiency of the proposed ILOA system shows 1.5 times (0.22%) of the conventional phased array (0.15%). It is noted that the two systems use the same transmit array for a fair comparison, whereas the conventional array has a separate RF front end connected to the antenna via a short coax cable with insertion loss of 1.3 dB in most cases. It is shown that in any RF transmitter, the block (oscillator or power amplifier), which converts DC to RF power with the most power consumption, has to be an efficient convertor and very last active block. Given similar power added efficiency of this block, the highly integrated ILOA design has higher transmission efficiency as it removes the lossy feed after amplification and utilizes the spatial power combining over the air.

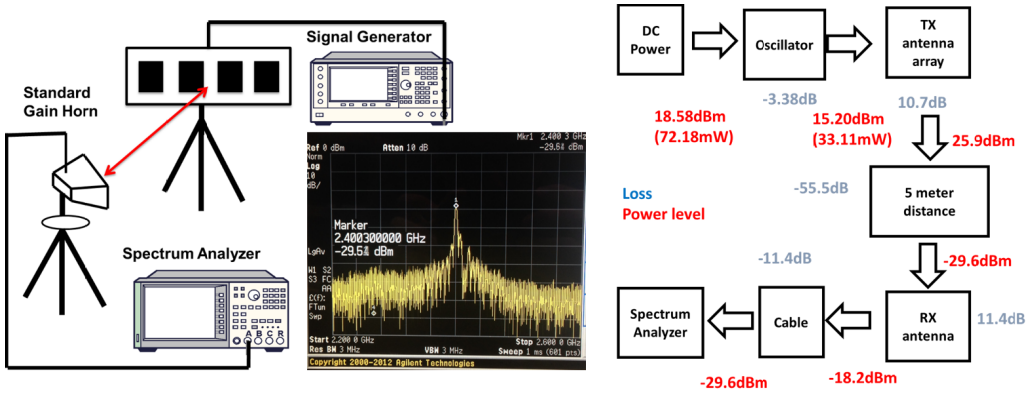

(a) (b)

Figure 8. (a) Injection-locked oscillator array experiment. (b) Link budget of the experiment.

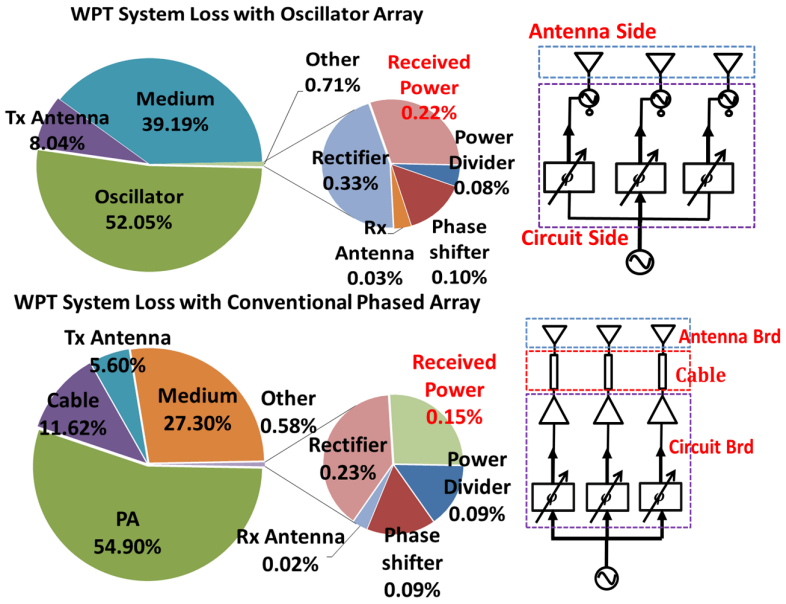

Figure 9. Estimated WPT sytem loss for ILOA and conventional phased array.

5. CONCLUSIONS

This paper presents a wireless power transmitter using the AIA technology at 2.4 GHz. This system minimizes the loss at the transmitter through spatial power combining and implements broader coverage and continuous scanning with additional discrete phase shift of injection signal. Our prototype is a scalable injection locked array that uses a multilayer substrate to make a compact and low-cost beamforming transmitter. Based on the experiment, the ILOA array shows the promise of upscaling to massive beamforming array with reduced hardware complexity and enhanced efficiency.

REFERENCES

1. Adler, R., "A study of locking phenomena in oscillators," *Proceedings of the IRE*, Vol. 34, No. 6, 351–357, 1946.
2. Birkeland, J. and T. Itoh, "A 16 element quasi-optical fet oscillator power combining array with external injection locking," *IEEE Transactions on Microwave Theory and Techniques*, Vol. 40, No. 3, 475–481, 1992.
3. Chen, J.-X., K. W. Lau, K. Y. Chan, C. H. K. Chin, Q. Xue, and C. H. Chan, "A double-sided parallel-strip line push-pull oscillator," *IEEE Microwave and Wireless Components Letters*, Vol. 18, No. 5, 335–337, 2008.
4. Choi, J., M. Nick, and A. Mortazawi, "Low phase-noise planar oscillators employing elliptic-response bandpass filters," *IEEE Transactions on Microwave Theory and Techniques*, Vol. 57, No. 8, 1959–1965, 2009.
5. Daryoush, A. S., "Optical synchronization of millimeter-wave oscillators for distributed architecture," *IEEE Transactions on Microwave Theory and Techniques*, Vol. 38, No. 5, 467–476, 1990.
6. Khanna, A. P. S., "Microwave oscillators: the state of the technology," *Microwave Journal*, Vol. 49, No. 4, 22, 2006.
7. Leeson, D. B., "A simple model of feedback oscillator noise spectrum," *Proceedings of the IEEE*, 329–330, 1966.
8. Massa, A., G. Oliveri, F. Viani, and P. Rocca, "Array designs for long-distance wireless power transmission: State-of-the-art and innovative solutions," *Proceedings of The IEEE*, Vol. 101, No. 6, 1464–1480, 2013.
9. McSpadden, J. O. and J. C. Mankins, "Space solar power programs and microwave wireless power transmission technology," *Microwave Magazine, IEEE*, Vol. 3, No. 4, 46–57, 2002.
10. Oida, A., H. Nakashima, J. Miyasaka, K. Ohdoi, H. Matsumoto, and N. Shinohara, "Development of a new type of electric off-road vehicle powered by microwaves transmitted through air," *Journal of Terramechanics*, Vol. 44, No. 5, 329–338, 2007.
11. Tseng, C.-H. and C.-L. Chang, "Design of low phase-noise microwave oscillator and wideband vco based on microstrip combline bandpass filters," *IEEE Transactions on Microwave Theory and Techniques*, Vol. 60, No. 10, 3151–3160, 2012.
12. York, R., T. Itoh, et al., "Injection-and phase-locking techniques for beam control [antenna arrays]," *IEEE Transactions on Microwave Theory and Techniques*, Vol. 46, No. 11, 1920–1929, 1998.